Application of a parameter-free Reggeized absorption model to spin-$2^{+}$ production



1973 J. Phys. A: Math. Nucl. Gen. 6 506

(http://iopscience.iop.org/0301-0015/6/4/015)

J. Phys. A: Gen. Phys., Vol. 5, April 1973. Printed in Great Britain. © 1973

# Application of a parameter-free reggeized absorption model to spin-2$^+$ production

P A Collins†, B J Hartley†, R W Moore‡ and K J M Moriarty§

† Department of Physics, Imperial College of Science and Technology, Prince Consort Road, London SW7, UK

‡ Department of Physics, Westfield College, Kidderpore Avenue, London NW3, UK

§ Department of Mathematics, Royal Holloway College, Englefield Green, Surrey, UK

MS received 9 February 1972, in revised form 8 September 1972

**Abstract.** A reggeized absorption model with no free parameters to be fitted to the data under consideration is applied to spin-2$^+$ production reactions. The differential cross section and spin density matrix elements are well represented by the model for pion dominated reactions but less well for processes not proceeding by pseudoscalar exchange.

## 1. Introduction

The importance of including Regge cut contributions to Regge amplitudes for two-body scattering processes is now generally recognized (Lovelace 1971). These cut contributions may be introduced by means of the absorption model in either of two currently popular versions, namely the so-called 'weak cut' model or the 'strong cut' model (Phillips 1970). The former has the advantages of containing wrong signature nonsense zeros in agreement with the Veneziano formula and of requiring less free parameters than the 'strong cut' model. By the incorporation of U(6,6) × O(3,1) symmetry in such a model, an absorption model which is essentially parameter free has been developed. This model has been discussed at length in a previous paper on meson–baryon scattering processes (Adjei *et al* 1971) and has also been applied to baryon–baryon scattering reactions (Adjei *et al* 1972).

Because of the current interest in spin-2$^+$ production reactions, both theoretically in terms of mechanisms for $A_2$ production (Michael and Runskanen 1971) and experimentally with the question of $A_2$ splitting (Grayer *et al* 1971), we have compared the predictions of this model with the experimental data now available on differential cross sections and density matrix elements.

In § 2, the formalism is developed, while in § 3 we conclude with a discussion of the results of the model as applied to reactions of the type $0^-\frac{1}{2}^+ \to 2^+\frac{1}{2}^+$ and $0^-\frac{1}{2}^+ \to 2^+\frac{3}{2}^+$ and which proceed by the exchange of nonstrange mesons.

## 2. Formalism

All freedom in the pole-graph amplitudes is eliminated by employing the U(6,6) × O(3,1) representation for the fields to construct the effective Lagrangians at the vertices of the

Born graphs. Thus, the ratio between the helicity amplitudes are fixed as are the ratios between the various contributions to a given reaction and the ratios between reactions for a given Born graph. This method of angular momentum excitation of the lowest representation allows the introduction of the $2^+$ fields which lie in the (6, $\bar{6}$, 1) without the introduction of exotics.

The effective Lagrangians are

$$L_{\bar{B}BM} = g\bar{B}^{(ABC)}B_{(ABD)}M^D_c$$

$$L_{MMM} = h[M, M']^B_A M^A_B$$

where $B$, $M$ and $M'$ are the fields corresponding to the (56, 1 : 0) baryon multiplet and the (6, $\bar{6}$, 0) and (6, $\bar{6}$ : 1) meson multiplets respectively, and $g$ and $h$ are the coupling constants.

Retaining just those parts of the currents which are of interest here (Delbourgo *et al* 1965) we have at the baryon vertex the pseudoscalar currents,

$$J_5(0) = g\left(1+\frac{2m}{\mu_0}\right)\left(1-\frac{t}{4m_B^2}\right)(\bar{N}\gamma_5 N)_{D+\frac{5}{3}F-S}$$

$$J_5(D) = g\left(1+\frac{2m}{\mu_0}\right)\frac{Q_\lambda}{\pi_B}(\bar{D}_\lambda N)_G$$

and the vector currents

$$J_\mu(0) = g\left[\frac{P_\mu}{2m_B}\left\{\left(1+\frac{\mu_0}{2m}\right)(\bar{N}N)_{F+3S}-\left(1+\frac{2m}{\mu_0}\right)(\bar{N}N)_{D+\frac{5}{3}F-S}\right\}\right.$$
$$\left.+\left(1+\frac{2m}{\mu_0}\right)\left(1-\frac{t}{4m_B^2}\right)(\bar{N}\gamma_\mu N)_{D+\frac{5}{3}F-S}\right]$$

$$J_\mu(D) = -\frac{g}{2m_B^2}\left(1+\frac{2m}{\mu_0}\right)\epsilon_{\mu\nu\kappa\lambda}P_\nu Q_\kappa(\bar{D}_\lambda N)_G$$

while at the meson vertex we have the pseudoscalar current

$$J_5(T) = -h\frac{\mu_1+2\mu_0}{2\mu_0^2}P'_\mu Q'_\nu(\bar{\phi}_{(\mu\nu)}\phi_5)_{D+2S}$$

and the vector current

$$J_\mu(T) = h\frac{\mu_1+2\mu_0}{4m_M^2\mu_0}P'_\eta\epsilon_{\mu\kappa\lambda\nu}P'_\lambda Q'_\nu(\bar{\phi}_{(\kappa\eta)}\phi_5)_F$$

where $P(P')$ and $Q(Q')$ are the sum and difference of the incoming and outgoing momenta at the baryon (meson) vertex, $D$, $F$, $S$ and $G$ are the symmetric, antisymmetric, singlet and decuplet U(3) couplings respectively.

For the group theoretic masses we have taken the baryon mass $m = 1{\cdot}27\ \mathrm{GeV}/c^2$, the average of the $\frac{1}{2}^+$ octet and $\frac{3}{2}^+$ decuplet, the mass associated with the (6, $\bar{6}$:0) $\mu_0 = 0{\cdot}63\ \mathrm{GeV}/c^2$ and the mass associated with the (6, $\bar{6}$:1) $\mu_1 = 1{\cdot}22\ \mathrm{GeV}/c^2$. Where shown we have used the average physical mass of the particles at the baryon and meson vertices, $m_B$ and $m_M$, respectively. In the evaluation of $\bar{N}N$ etc we use the physical masses of the particles. This mass splitting prescription is fully consistent with the one adopted previously (Adjei *et al* 1971, 1972).

The baryon–baryon–meson coupling constant is obtained from the known pion–nucleon coupling constant (Ebel *et al* 1969)

$$\frac{g_{NN\pi}^2}{4\pi} = 14{\cdot}9 = \frac{g^2}{4\pi}\left(1+\frac{2m}{\mu_0}\right)^2\left(1-\frac{m_\pi^2}{4m_{\mathrm{B}}^2}\right)\left(\frac{5}{3}\right)^2$$

while the meson–meson–meson coupling constant is determined from the $f^0 \to \pi^+\pi^-$ decay width (Particle Data Group 1970):

$$\Gamma_{f^0\to\pi^-\pi^-} = \frac{|\boldsymbol{p}|}{2m_{f^0}^2}\frac{1}{4\pi}\overline{\sum_{\text{spins}}}|T|^2 = \frac{h^2|\boldsymbol{p}|^5}{30\pi m_{f^0}^2}\frac{(\mu_1+2\mu_0)^2}{\mu_0^4}$$

where $\boldsymbol{p}$ is the CM three-momentum of the decay products. The value of the mass $\mu_1$ is, in fact, irrelevant, since it cancels using this relation.

The one-particle-exchange diagrams are then calculated using second order perturbation theory. For pseudoscalar exchange the $T$ matrix is

$$T_{\mathrm{p}} = \left\langle p_3p_4 \left| J_5'\frac{1}{t-M^2}J_5 \right| p_1p_2 \right\rangle$$

and for the vector exchange

$$T_{\mathrm{v}} = \left\langle p_3p_4 \left| J_\mu'\frac{-g_{\mu\nu}+Q_\mu Q_\nu/M^2}{t-M^2}J_\nu \right| p_1p_2 \right\rangle$$

where the primed and unprimed currents distinguish the two vertices, $M$ is the mass of the exchanged particle and the diagonal metric is $g_{\mu\nu} = (+1;-1,-1,-1)$.

Reggeization is accomplished by the replacement

$$\frac{1}{t-M^2} \to -\alpha'\Gamma(-\alpha)\frac{1+\exp(-\mathrm{i}\pi\alpha)}{2}\left(\frac{s+\frac{1}{2}t-\frac{1}{2}\Sigma_i m_i^2}{s_0}\right)^{\alpha}$$

for pseudoscalar exchange and

$$\frac{1}{t-M^2} \to -\alpha'\Gamma(1-\alpha)\frac{1-\exp(-\mathrm{i}\pi\alpha)}{2}\left(\frac{s+\frac{1}{2}t-\frac{1}{2}\Sigma_i m_i^2}{s_0}\right)^{\alpha-1}$$

for vector exchange, where $s_0$ is the scale factor assumed to be 1 $\mathrm{GeV}^2$. The Gell-Mann ghost eliminating mechanism has been employed (Adjei *et al* 1970).

The $1^+$ and $2^+$ exchanges are introduced by changing the signature and Clebsch–Gordan coefficients of the $0^-$ and $1^-$ exchanges respectively, with the assumption of strong exchange degeneracy to determine the coupling strength. The amplitude for $0^-\frac{1}{2}^+ \to 2^+\frac{1}{2}^+$ then becomes

$$T_{\mathrm{p}} = \frac{gh(\mu_1+2\mu_0)}{2\mu_0^2}\left(1+\frac{2m}{\mu_0}\right)\left(1-\frac{t}{4m_{\mathrm{B}}^2}\right)\alpha'\Gamma(-\alpha)\left(\frac{1+\exp(-\mathrm{i}\pi\alpha)}{2}\right)\left(\frac{s+\frac{1}{2}t-\frac{1}{2}\Sigma_i m_i^2}{s_0}\right)^{\alpha}$$
$$\times P_\mu'Q_\nu'(\bar{\phi}_{(\mu\nu)}\phi_5)_{D+2S}(\bar{N}\gamma_5 N)_{D+\frac{3}{5}F-S}$$

$$T_v = \frac{gh(\mu_1+2\mu_0)}{4m_M^2\mu_0}\alpha'\Gamma(1-\alpha)\left(\frac{1-\exp(-i\pi\alpha)}{2}\right)\left(\frac{s+\frac{1}{2}t-\frac{1}{2}\Sigma_i m_i^2}{s_0}\right)^{\alpha-1} P'_\mu\epsilon_{\kappa\nu\sigma\rho}P'_\sigma Q'_\rho(\bar{\Phi}_{(\mu\nu)}\phi_5)_F$$
$$\times\left[\frac{P_\kappa}{2m_B}\left\{\left(1+\frac{\mu_0}{2m_B}\right)(\bar{N}N)_{F+3S}-\left(1+\frac{2m}{\mu_0}\right)(\bar{N}N)_{D+\frac{1}{3}F-S}\right\}+\left(1+\frac{2m}{\mu_0}\right)\right.$$
$$\left.\times\left(1-\frac{t}{4m_B^2}\right)(\bar{N}\gamma_\kappa N)_{D+\frac{1}{3}F-S}\right]$$

while the amplitude for $0^-\frac{1}{2}^+ \to 2^+\frac{3}{2}^+$ becomes

$$T_p = gh\frac{(\mu_1+2\mu_0)}{2\mu_0^2}\left(1+\frac{2m}{\mu_0}\right)\alpha'\Gamma(-\alpha)\left(\frac{1+\exp(-i\pi\alpha)}{2}\right)\left(\frac{s+\frac{1}{2}t-\frac{1}{2}\Sigma_i m_i^2}{s_0}\right)^{\alpha} P'_\mu Q'_\nu\frac{Q_\kappa}{m_B}$$
$$\times(\bar{\Phi}_{(\mu\nu)}\phi_5)_{D+2S}(\bar{D}_\kappa N)_G$$

$$T_v = -gh\frac{(\mu_1+2\mu_0)}{8m_B^2\mu_0 m_M^2}\left(1+\frac{2m}{\mu_0}\right)\alpha'\Gamma(1-\alpha)\left(\frac{1-\exp(-i\pi\alpha)}{2}\right)\left(\frac{s+\frac{1}{2}t-\frac{1}{2}\Sigma_i m_i^2}{s_0}\right)^{\alpha-1} P'_\mu\epsilon_{\kappa\nu\sigma\rho}\epsilon_{\kappa\eta\alpha\lambda}$$
$$\times P'_\sigma Q'_\rho P_\eta Q_\alpha(\bar{\Phi}_{(\mu\nu)}\phi_5)_F(\bar{D}_\lambda N)_G.$$

The $s$ channel helicity amplitudes in the centre-of-mass frame for $0^-\frac{1}{2}^+ \to 2^+\frac{1}{2}^+$ are given in appendix 1, while those for $0^-\frac{1}{2}^+ \to 2^+\frac{3}{2}^+$ are given in appendix 2.

The Regge trajectories, taken to be linear, were obtained by constraining them to pass through the positions of the relevant particles on the Chew–Frautschi plot with π–B, ρ–$A_2$ and ω–$f^0$ exchange degeneracy. This gives for the π–B trajectory

$$a(t) = -0{\cdot}013+0{\cdot}665t$$

for the ρ–$A_2$ trajectory

$$a(t) = 0{\cdot}470+0{\cdot}905t$$

and for the ω–$f^0$ trajectory

$$a(t) = 0{\cdot}386+1{\cdot}017t.$$

To introduce the absorption corrections the $s$ channel helicity amplitudes are first expanded in partial wave series

$$\langle\lambda_3\lambda_4|\phi(s,t)|\lambda_1\lambda_2\rangle = \sum_{j=j_{\min}}^{\infty}(2j+1)\langle\lambda_3\lambda_4|T^j(s)|\lambda_1\lambda_2\rangle d^j_{\lambda\mu}(\cos\theta)$$

where $j$ is the total angular momentum, $j_{\min} = \max(|\lambda|, |\mu|)$, $\theta$ is the CM scattering angle, $\lambda = \lambda_1-\lambda_2$, $\mu = \lambda_3-\lambda_4$ and the partial wave amplitudes are given by

$$\langle\lambda_3\lambda_4|T^j(s)|\lambda_1\lambda_2\rangle = \tfrac{1}{2}\int_{-1}^{+1}\langle\lambda_3\lambda_4|\phi(s,t)|\lambda_1\lambda_2\rangle d^j_{\lambda\mu}(\cos\theta)\,\mathrm{d}(\cos\theta).$$

We then employ the Watson absorption formulae (Adjei *et al* 1971), simplified by the assumption that the elastic scattering is pure helicity nonflip. According to this prescription, the modified partial wave amplitudes are given by

$$\langle\lambda_3\lambda_4|T'^j(s)|\lambda_1\lambda_2\rangle = \tfrac{1}{2}(S^{\mathrm{el}j}_{\mathrm{final}}+S^{\mathrm{el}j}_{\mathrm{initial}})\langle\lambda_3\lambda_4|T^j(s)|\lambda_1\lambda_2\rangle$$

where $S^{\mathrm{el}j}$ is the $S$ matrix element for elastic scattering in the initial or final state. This is parametrized by a real gaussian form

$$S^{elj} = 1 - C\exp\left(\frac{-j(j+1)}{R^2P^2}\right)$$

where $P$ is the CM three-momentum. The coefficients $R$ and $C$, assumed the same in the final state as in the initial state, were determined from the observed experimental slope of the elastic scattering for small angles

$$\frac{(\mathrm{d}\sigma/\mathrm{d}t)_{el}}{(\mathrm{d}\sigma/\mathrm{d}t)_{el}}\bigg|_{t=0} = \exp(\tfrac{1}{2}R^2t)$$

and the optical theorem, which gives

$$C = \frac{\sigma_{tot}}{2\pi R^2}.$$

The values obtained (Adjei *et al* 1971) are given in table 1.

**Table 1.** Absorption coefficients

| Channel | $P_{lab}$ (GeV/$c$) | $C$ | $R^{-1}$ (GeV/$c$) |
|---|---|---|---|
| $\pi^-$p | 4·0 | 0·84 | 0·26 |
| | 7·0 | 0·78 | 0·26 |
| | 8·0 | 0·76 | 0·26 |
| | 11·0 | 0·73 | 0·26 |
| | 17·2 | 0·70 | 0·26 |
| $\pi^+$p | 4·0 | 0·87 | 0·27 |
| | 8·0 | 0·78 | 0·27 |
| | 13·1 | 0·74 | 0·27 |
| | 18·5 | 0·72 | 0·27 |
| $K^-$p | 4·1 | 0·77 | 0·26 |
| | 5·5 | 0·73 | 0·26 |
| | 10·0 | 0·66 | 0·26 |

The partial wave series are then resummed to obtain the modified $s$ channel helicity amplitudes, from which the differential cross section and density matrix elements are evaluated (Jackson *et al* 1965, Pilkuln and Svensson 1965). This work was performed numerically (Adjei *et al* 1970).

## 3. Discussion and results

The reactions of the type $0^-\frac{1}{2}^+ \to 2^+\frac{1}{2}^+$ which we have considered are

$$\pi^-\mathrm{p} \to \mathrm{f}^0\mathrm{n}$$

$$\mathrm{K}^-\mathrm{p} \to \mathrm{K}^{**-}\mathrm{p}$$

$$\mathrm{K}^-\mathrm{p} \to \overline{\mathrm{K}}^{**0}\mathrm{n}$$

$$\pi^+\mathrm{p} \to \mathrm{A}_2^+\mathrm{p}$$

$$\pi^-\mathrm{p} \to \mathrm{A}_2^-\mathrm{p}.$$

We have also performed calculations on two reactions of the type $0^-\frac{1}{2}^+ \to 2^+\frac{3}{2}^+$, namely

$$\pi^+ p \to f^0 \Delta^{++}$$

$$\pi^+ p \to A_2^0 \Delta^{++}.$$

We have considered differential cross sections for the above reactions, together with the density matrix elements in the Jackson frame where available.

The predicted differential cross section for the reaction $\pi^- p \to f^0 n$ from $\pi$ exchange is compared in figure 1 with the data (ABBHLM 1964, Poirier *et al* 1967, Caso *et al* 1969), which has been renormalized using smoothed total cross sections (Flaminio *et al* 1970).

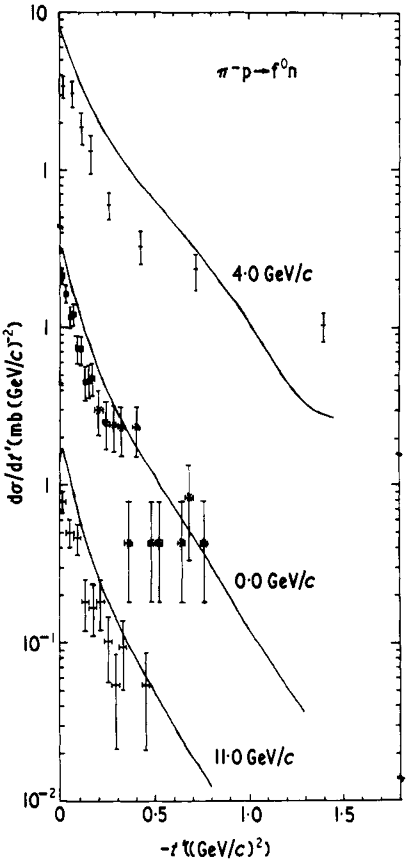


**Figure 1.** Differential cross section for $\pi^- p \to f^0 n$. Data from ABBHLM (1964), Poirier *et al* (1967) and Caso *et al* (1969).

Although the normalization given by the model is too large, this could be rectified by changing the decay width for $f^0 \to \pi^+\pi^-$ within the experimental error. The $s$ and $t$ dependence of the model are consistent with experiment. The density matrix elements of the $f^0$ resonance from $\pi$ exchange are shown in figures 2 and 3 (Poirier *et al* 1967, ABC 1966). The model agrees with the data for the elements $\rho_{00}$ and $\rho_{2,-2}$, but not for $\rho_{11}$ and $\rho_{22}$. The negative value of $\rho_{22}$, which is not consistent with $t$ channel

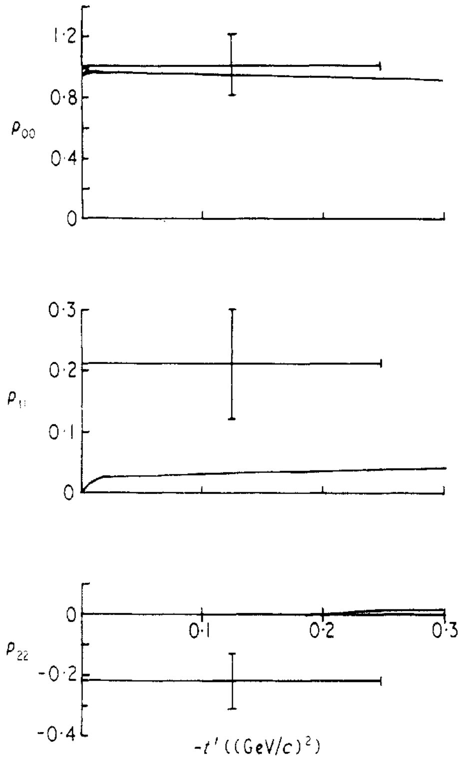


**Figure 2.** Density matrix elements of the $f^0$ resonance in $\pi^- p \to f^0 n$ at 4·0 GeV/$c$. Data from ABC (1966).

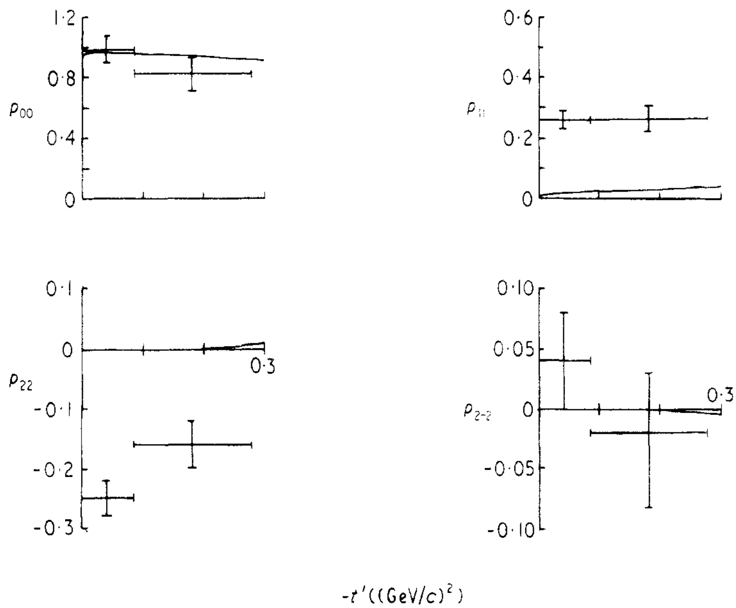


**Figure 3.** Density matrix elements of the $f^0$ resonance in $\pi^- p \to f^0 n$ at 8·0 GeV/$c$. Data from ABBHLM (1964).

particle exchange, is thought to be an *s* wave interference effect (ABC 1966). The inclusion of $A_2$ exchange gives a differential cross section which is too broad and does not help to improve the agreement with the density matrix data. Although a relatively large coupling for the $A_2$ is predicted by the symmetry scheme, experimentally, the coupling is small since $f^0$ decays almost entirely into $\pi^+\pi^-$ (Particle Data Group 1970). For these reasons we have omitted $A_2$ exchange in this reaction. For consistency, we have also omitted it from all other reactions in this group.

In a previous publication (Adjei *et al* 1971) we included the $A_2$ exchange. However, the application to $\rho$ production showed that in certain processes the $A_2$ contribution was too large leading to poor wide angle behaviour. This appears to indicate that U(6, 6) × O(3, 1) symmetry combined with exchange degeneracy is not a good approximation for certain $A_2$ couplings.

The contributions to the differential cross section for the reaction $K^-p \rightarrow K^{**-}p$ at 10 GeV/*c* (ABCLV 1968) from $\pi$, $\rho$, $\omega$ and $f^0$ exchange and their sum are shown in figure 4. This illustrates the predicted pion dominance near the forward direction with vector exchange dominance at wider angles. Figure 5 shows the energy dependence of the differential cross section for this reaction. The normalization of the data at 4·1,

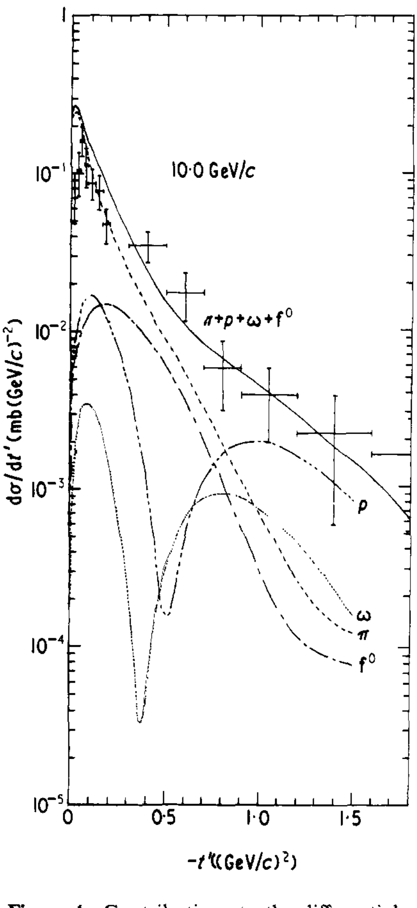


**Figure 4.** Contributions to the differential cross section for $K^-p \rightarrow K^{**-}p$ from $\pi$, $\rho$, $\omega$, $f^0$ and $\pi+\rho+\omega+f^0$ exchanges. Data from ABCLV (1968).

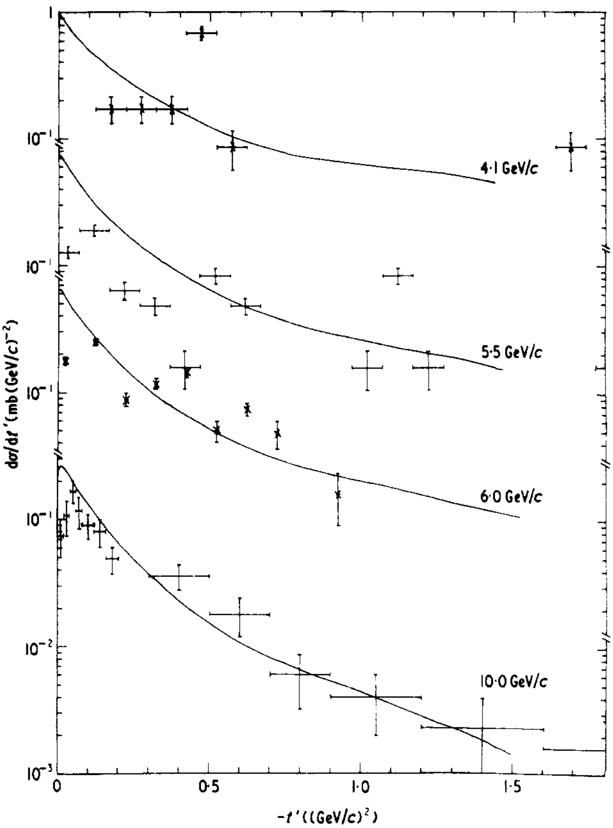


**Figure 5.** Differential cross section for $K^-p \rightarrow K^{**-}p$. Data from ABCLV (1968), Schweingruber *et al* (1968) and BGLMOR (1968).

5·5 and 6·0 GeV/$c$, (Schweingruber *et al* 1968, BGLMOR 1968) has been adjusted using smoothed total cross sections (Flaminio *et al* 1970). Although the data is extremely poor, except at 10·0 GeV/$c$, the normalization given by the model appears to be too large in the forward direction.

The predictions for the density matrix elements of the K** resonance are shown in figures 6 and 7. Although the data is poor, the large value of $\rho_{00}$ and small value of $\rho_{1,-1}$ confirms pion dominance near the forward direction.

An improved fit to both the differential cross section data and to the density matrix data could probably be obtained if the ratio of the pion contribution to the other contributions was decreased. The differential cross section turnover would then be lower and wider in the forward direction, and the density matrix element predictions would still be equally compatible with the data as now.

As explained elsewhere, the $\eta$, $A_2$ and B have been neglected here.

In figures 8 and 9 respectively, the differential cross sections (ABCLV 1968, Schweingruber *et al* 1968) and one-particle density matrix elements for $K^-p \rightarrow \overline{K}^{**0}n$ are shown. The model gives similar results to those for $K^-p \rightarrow K^{**-}p$, but here, at low energies and wide angles, the differential cross section data has a secondary maximum which is not reproduced although the theoretical prediction flattens out.

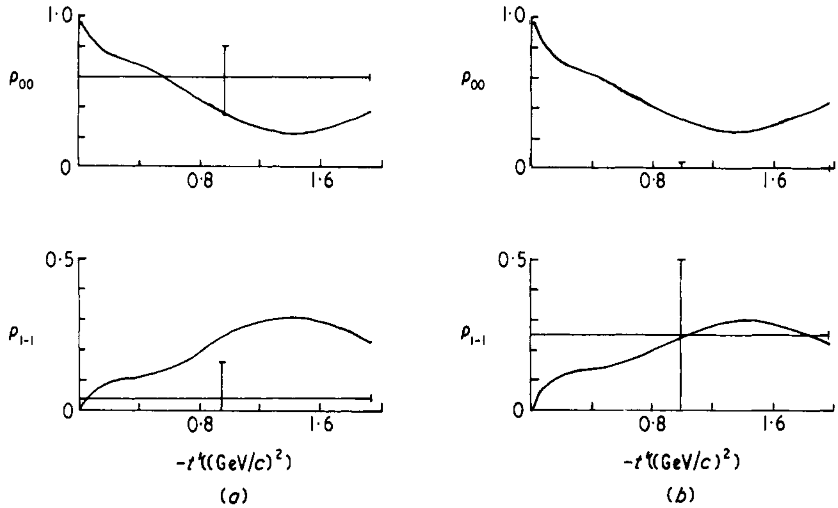


**Figure 6.** Density matrix elements of the K** resonance in $K^-p \to K^{**-}p$ at (*a*) 4·1 GeV/*c* and (*b*) 5·5 GeV/*c*. Data from Schweingruber *et al* (1968).

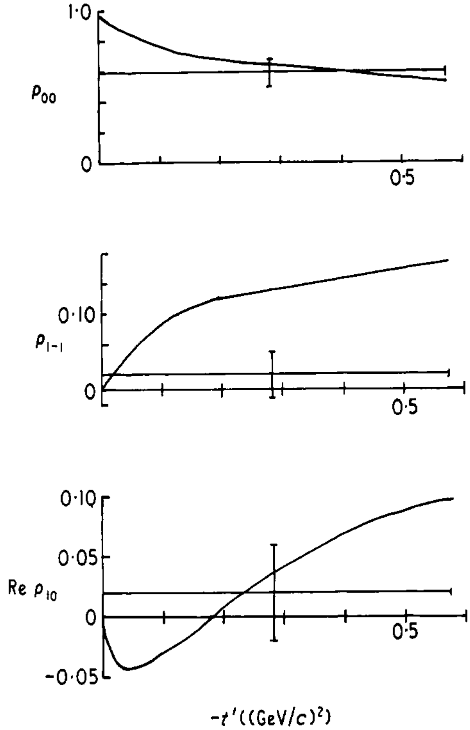


**Figure 7.** Density matrix elements of the K** resonance in $K^-p \to K^{**-}p$ at 6·0 GeV/*c*. Data from BGLMOR (1968).

The prediction at 10 GeV/*c* does not give the correct normalization for the differential cross section data, which appears to be at variance with the SU(3) prediction from $K^-p \to K^{**-}p$.

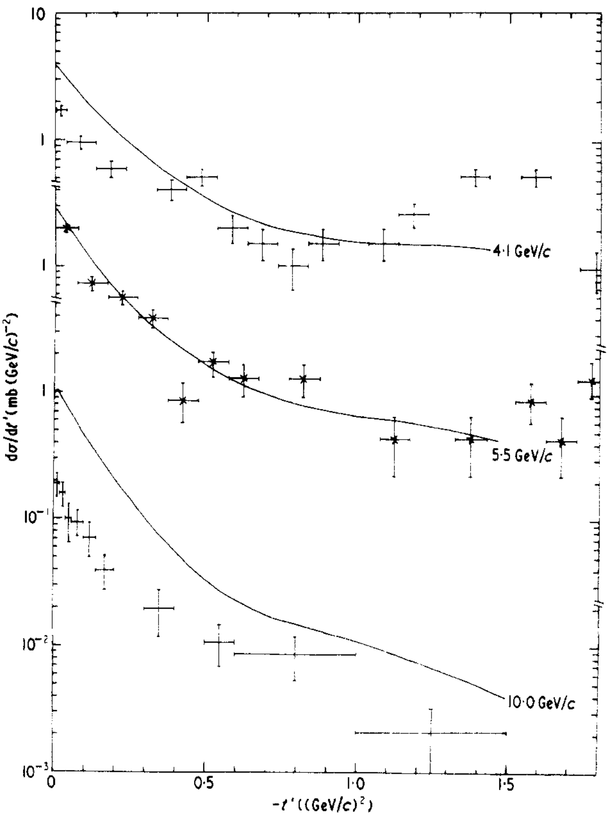


**Figure 8.** Differential cross section for $K^-p \to \overline{K}^{**0}n$. Data from ABCLV (1968) and Schweingruber *et al* (1968).

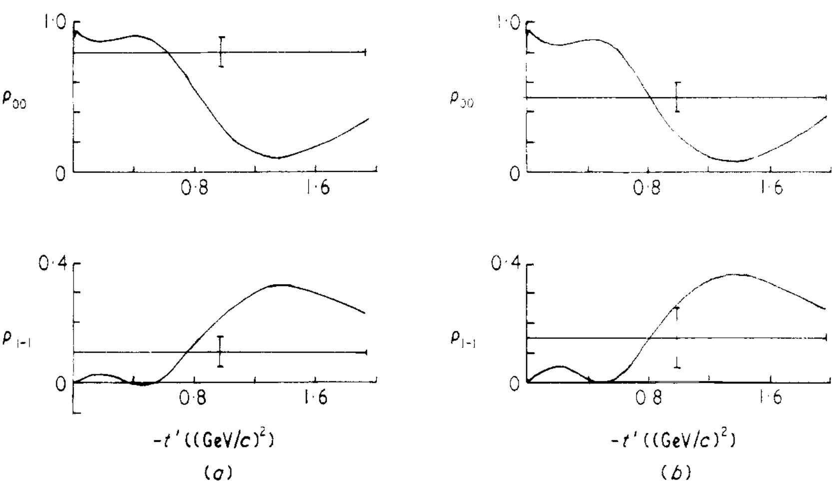


**Figure 9.** Density matrix elements of the $\overline{K}^{**}$ resonance in $K^-p \to \overline{K}^{**0}n$. Data from Schweingruber *et al* (1968).

The $\rho$ and $f^0$ contributions to the differential cross section for $\pi^+ p \rightarrow A_2^+ p$ at 8 GeV/$c$ are shown in figure 10. The $\rho$ and $f^0$ are similar in magnitude near the forward direction, but the $\rho$ dominates at wider angles. For this reaction and for $\pi^- p \rightarrow A_2^- p$, the $\eta$ and B (ie unnatural parity) exchange have been neglected as the $\eta$ gives a very small contribution due to its low lying trajectory while the B is neglected as $\rho_{00}$ for $\pi^- p \rightarrow A_2^- p$ has a small value which indicates natural parity dominance.

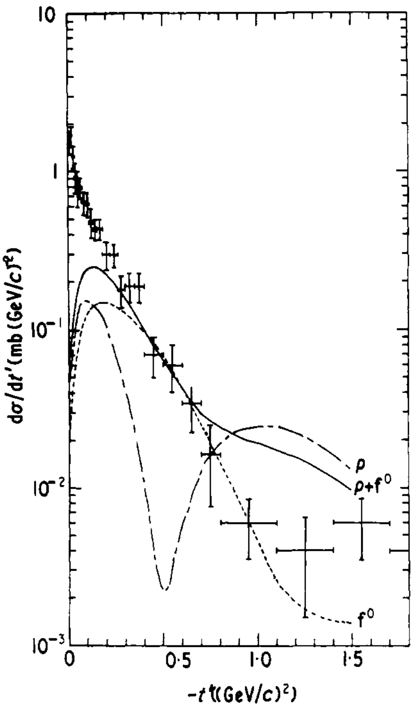


**Figure 10.** Contributions to the differential cross section for $\pi^+ p \rightarrow A_2^+ p$ at 8·0 GeV/$c$ from $\rho$ and $f^0$ exchanges. Data from ABBBHLM (1965).

Figure 11, 12 and 13 (ABBBHLM 1965, ABC 1968, Johnson *et al* 1970, Grayer *et al* 1971) illustrate the differential cross sections for $\pi^+ p \rightarrow A_2^+ p$, $\pi^- p \rightarrow A_2^- p$ and the one-particle decay density matrix elements for the $A_2^-$, respectively. While the density matrix elements are consistent with natural parity exchange, the differential cross section predictions turn over in the forward direction in contrast to the presently available lower energy data which peaks, but consistent with the new $\pi^- p \rightarrow A_2^- p$ data at 17·2 GeV/$c$ (Grayer *et al* private communication). Another anomaly also exists in $\pi^+ p \rightarrow A_2^+ p$ as the 4 GeV/$c$ has a smaller normalization than the 8 GeV/$c$ data resulting in too much wide angle scattering in our prediction at this lower energy.

There are two currently available explanations for this 'diffractive-like' peak, at the lower energies, if it indeed does exist. Firstly, if one believes in the Morrison rule for a process to proceed by pomeron exchange in the $t$ channel then,

$$P_f = P_i(-1)^{\Delta J}$$

where $\Delta J$ is the change of spin between the incident particle of parity $P_i$ and the final

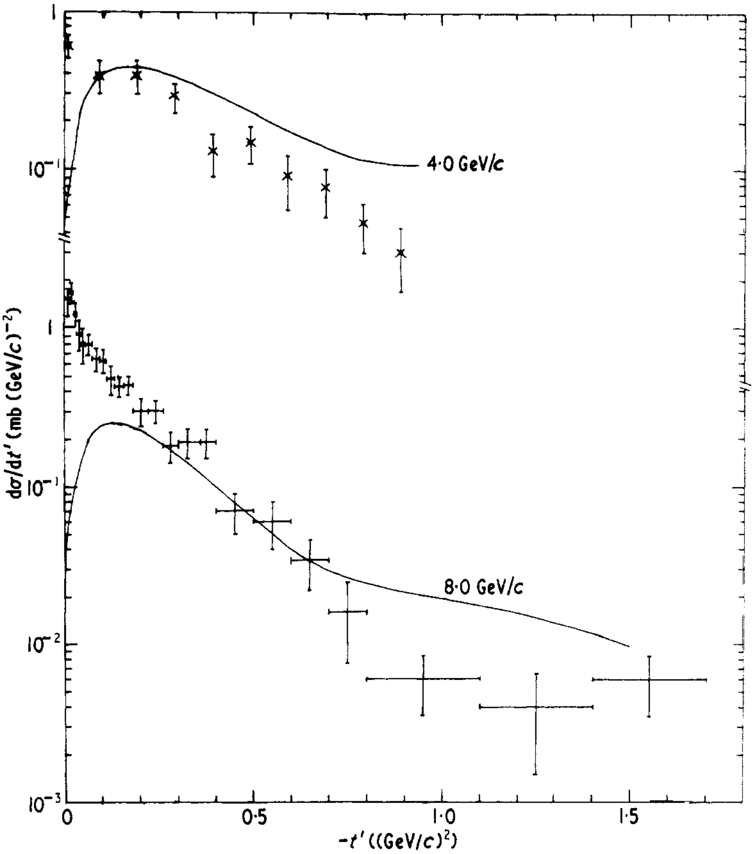


**Figure 11.** Differential cross section for $\pi^+ p \to A_2^+ p$. Data from ABBBHLM (1965) and ABC (1968).

one of parity $P_f$. This is not valid at the $\pi$–$A_2$ vertex, so the peak is assumed to be a 'Deck-effect' background.

The second explanation is that of Freund *et al* (1971). Here, the Morrison rule is disregarded and the $t$ channel pomeron is constructed from a 'twisted loop' quark diagram which couples as the U(3) singlet combination of $f^0$ and $f'$. Hence the pomeron couples to $\pi^{\pm} p \to A_2^{\pm} p$ and could account for the peak. However, the experimental evidence on which this latter suggestion is based, seems rather dubious. The total cross section data for $\pi^- p \to A_2^- p$ has poor statistics and there appears to be no evidence for pomeron exchange in KN → K**N.

With the higher energy data at 17·2 GeV/$c$ for $\pi^- p \to A_2^- p$ the points are a preliminary analysis of $A_2^- \to K^- K^0$ and the normalization is arbitrary, but as stated before, a forward turnover definitely exists.

The reaction $\pi^+ p \to f^0 \Delta^{++}$ has its differential cross section illustrated in figure 14 (ABC 1968, Biswas *et al* 1970), and the one-particle decay density matrix elements for the $f^0$ and $\Delta^{++}$ are shown in figures 15, 16, 17, 18 and 19 (Gaidos *et al* 1971, Biswas *et al* 1970, ABC 1970). The features of the differential cross sections are equally well represented by just $\pi$ exchange or $\pi + A_2$ exchange. However, while the addition of the $A_2$ improved the $\rho_{00}$, $\rho_{11}$ and Re $\rho_{10}$ density matrix elements, it made $\rho_{1,-1}$, Re $\rho_{20}$, Re $\rho_{21}$

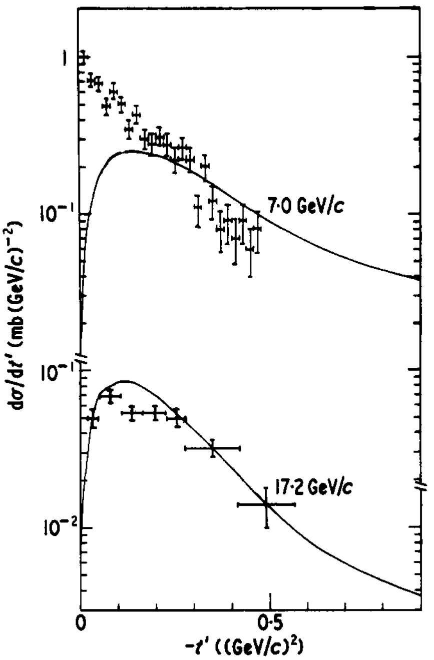


**Figure 12.** Differential cross section for $\pi^- p \to A_2^- p$. Data from Johnson *et al* (1970) and Grayer *et al* (private communication).

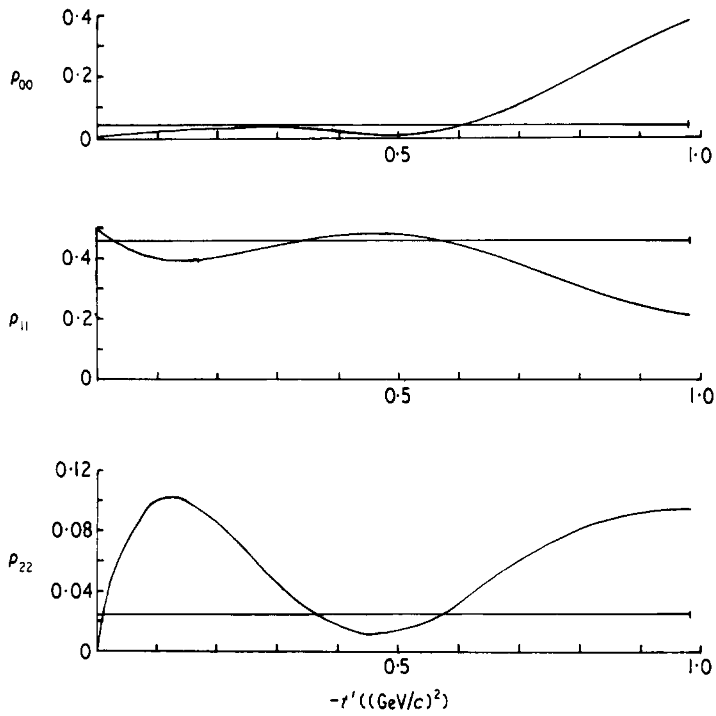


**Figure 13.** Density matrix elements of the $A_2$ resonance in $\pi^- p \to A_2^- p$ at 7·0 GeV/*c*. Data from Johnson *et al* (1970).

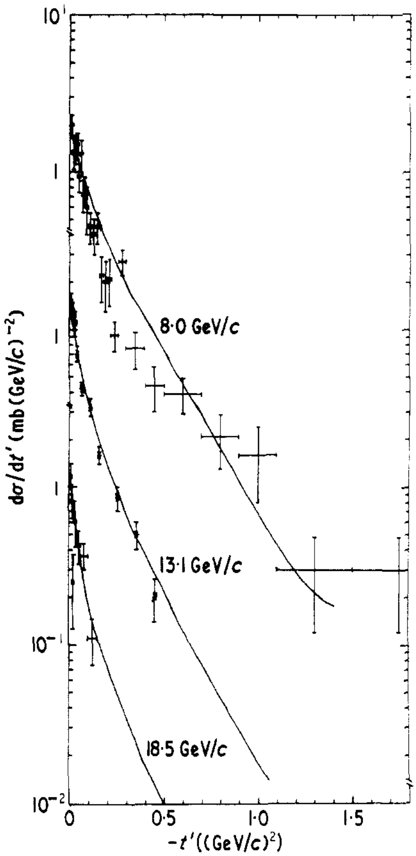


**Figure 14.** Differential cross section for $\pi^+ p \to f^0 \Delta^{++}$. Data from ABC (1968), Gaidos *et al* (1971) and Biswas *et al* (1970).

and Re $\rho_{3,-1}$ worse. Hence, for consistency with $\pi^- p \to f^0 n$, the $A_2$ exchange was omitted although Gaidos *et al* (1971) claim to see a small bump in their cos $\theta_J$ distribution at cos $\theta_J = 0$ which is typical of $A_2$ exchange. However, they show that this $A_2$ contribution has a small effect on the differential cross section.

The last reaction to be treated was $\pi^+ p \to A_2^0 \Delta^{++}$, for which the $\rho$, B and $\rho + B$ contributions to the differential cross sections at 8 GeV/$c$ are shown in figure 20 (ABC 1968). Here, no diffractive-like peak is present in the forward direction so the differential cross section data dip towards $t = 0$. However, the differential cross section still rises too quickly to be compatible with our model which predicts B dominance and so gives a flat distribution.

Better agreement with the data could be obtained if we had a larger $\rho$ contribution. This is obtained using the same input in $\pi N \to \omega N$ and $\pi N \to \omega \Delta^{++}$ but here the kinematics upset this ansatz.

In conclusion, we find that our model is quite satisfactory for pion dominated reactions. However, for $A_2$ production reactions, the density matrix elements are consistent with our model although there is a disagreement with the differential cross section data as we do not obtain any 'diffractive-like' peaks.

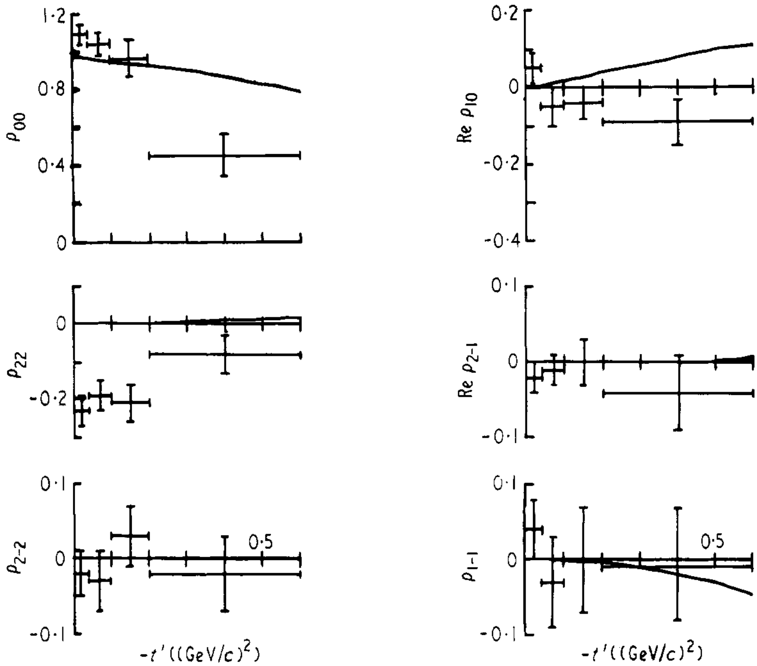


**Figure 15.** Density matrix elements of the $f^0$ resonance in $\pi^+ p \to f^0 \Delta^{++}$ at 8·00 GeV/$c$. Data from ABC (1970).

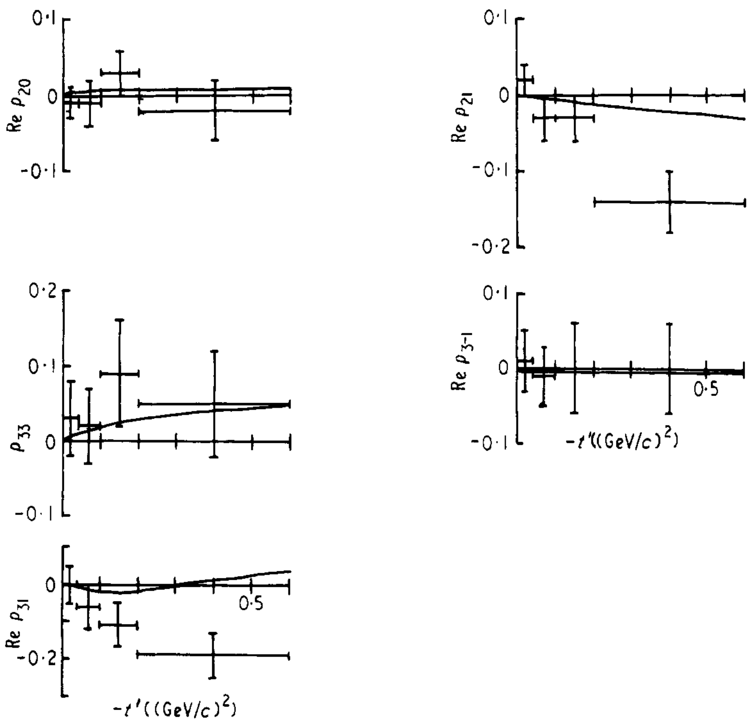


**Figure 16.** Density matrix elements of the $f^0$ and $\Delta$ resonances in $\pi^+ p \to f^0 \Delta^{++}$ at 8·0 GeV/$c$. Data from ABC (1970).

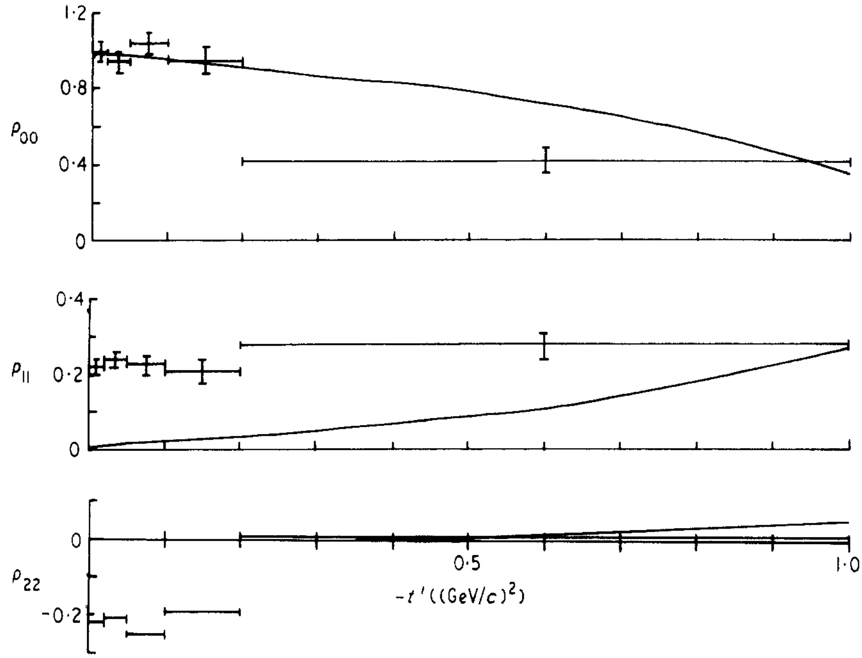


**Figure 17.** Density matrix elements of the $f^0$ resonance in $\pi^+ p \to f^0 \Delta^{++}$ at 13·1 GeV/c. Data from Gaidos *et al* (1971).

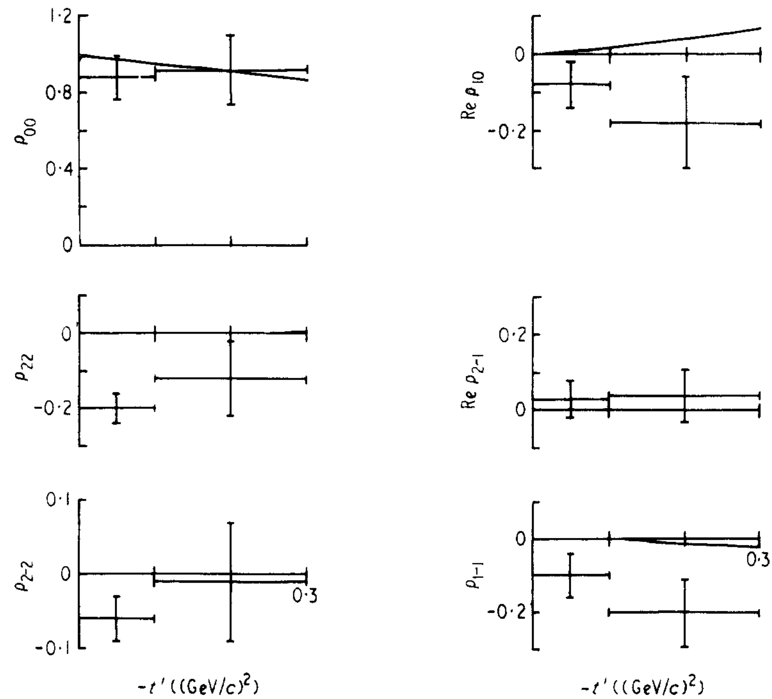


**Figure 18.** Density matrix elements of the $f^0$ resonance in $\pi^+ p \to f^0 \Delta^{++}$ at 18·5 GeV/c. Data from Biswas *et al* (1970).

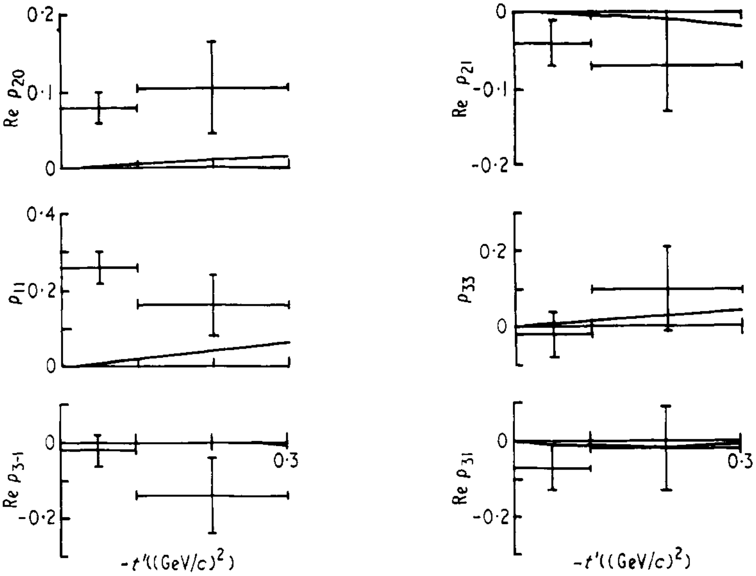


**Figure 19.** Density matrix elements of the $f^0$ and $\Delta$ resonances in $\pi^+p \to f^0\Delta^{++}$ at 18·5 GeV/$c$. Data from Biswas *et al* (1970).

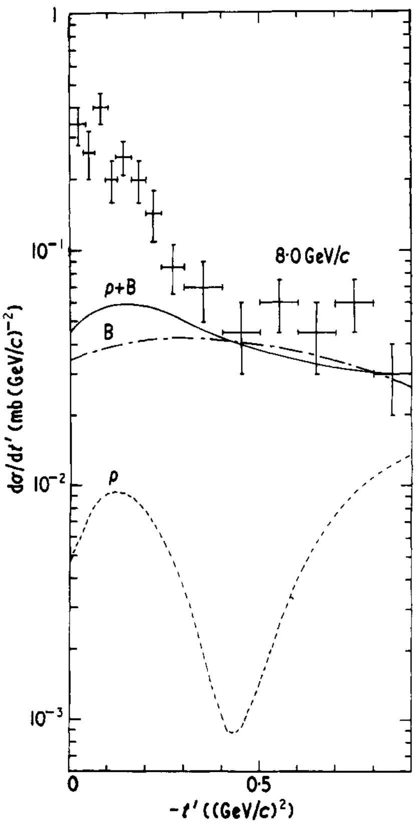


**Figure 20.** Contributions to the differential cross section for $\pi^+p \to A_2^0\Delta^{++}$ from $\rho$ and B exchanges. Data from ABC (1968).

**Acknowledgments**

We are indebted to Professor M H Ross for a critical reading of the manuscript and wish to thank the Science Research Council for financial support.

## Appendix 1

The $s$ channel helicity amplitudes for $0^-\frac{1}{2}^+ \rightarrow 2^+\frac{1}{2}^+$ are evaluated in the centre-of-mass frame. Parity invariance relations reduce the number of independent amplitudes to ten. These relations are shown in table 2.

**Table 2.** Relations between $s$ channel helicity amplitudes for $0^-\frac{1}{2}^+ \rightarrow 2^+\frac{1}{2}^+$ given by parity invariance

| $\lambda_4$ | $\lambda_3$ \ $\lambda_2\ \lambda_1$ | $\frac{1}{2}$ 0 | $-\frac{1}{2}$ 0 |
|---|---|---|---|
| $\frac{1}{2}$ | 2 | $\phi_1$ | $\phi_6$ |
| $\frac{1}{2}$ | 1 | $\phi_2$ | $\phi_7$ |
| $\frac{1}{2}$ | 0 | $\phi_3$ | $\phi_8$ |
| $\frac{1}{2}$ | $-1$ | $\phi_4$ | $\phi_9$ |
| $\frac{1}{2}$ | $-2$ | $\phi_5$ | $\phi_{10}$ |
| $-\frac{1}{2}$ | 2 | $\phi_{10}$ | $-\phi_5$ |
| $-\frac{1}{2}$ | 1 | $-\phi_9$ | $\phi_4$ |
| $-\frac{1}{2}$ | 0 | $\phi_8$ | $-\phi_3$ |
| $-\frac{1}{2}$ | $-1$ | $-\phi_7$ | $\phi_2$ |
| $-\frac{1}{2}$ | $-2$ | $\phi_6$ | $-\phi_1$ |

In order to write down the helicity amplitudes, we define suffices 1, 2, 3, 4 for the incoming meson and baryon and the outgoing meson and baryon respectively. $s, t, u$ are the Mandelstam variables. $m_i$, $E_i$, $i = 1, \ldots, 4$ are the masses and CM energies respectively. $K(Q)$ are the incoming (outgoing) CM momenta.

$$C = \{(E_1+m_1)(E_3+m_3)\}^{1/2}$$

$\theta$ is the CM scattering angle

$$\beta_{\mathrm{p}} = gh\frac{(\mu_1+2\mu_0)}{2\mu_0^2}\left(1+\frac{2m}{\mu_0}\right)\alpha'\Gamma(-\alpha)\left(\frac{1+\exp(-\mathrm{i}\pi\alpha)}{2}\right)\left(\frac{s+\frac{1}{2}t-\frac{1}{2}\Sigma_i m_i^2}{s_0}\right)^{\alpha}$$

$$\beta_{\mathrm{v}} = gh\frac{(\mu_1+2\mu_0)}{4m_{\mathrm{M}}^2\mu_0}\alpha'\Gamma(1-\alpha)\left(\frac{1-\exp(-\mathrm{i}\pi\alpha)}{2}\right)\left(\frac{s+\frac{1}{2}t-\frac{1}{2}\Sigma_i m_i^2}{s_0}\right)^{\alpha-1}$$

$h_{D+2S}, h_F$, are the U(3) couplings at the meson vertex. $g_{F+3S}, g_{D+\frac{1}{3}F-S}, G$ are the U(3) couplings at the baryon vertex.

$$a_{\pm} = \frac{Q}{E_4+m_4} \pm \frac{K}{E_2+m_2}$$

$$b_{\mathrm{p}} = h_{D+2S}g_{D+\frac{1}{3}F-S}\left(1-\frac{t}{4m_{\mathrm{B}}^2}\right)$$

$$l = E_1 Q - E_3 K \cos\theta$$

$$W = E_1 + E_2 = E_3 + E_4, \qquad \text{the CM energy}$$

$$b_v = \frac{h_F}{m_B}\left\{\left(1+\frac{\mu_0}{2m}\right)g_{F+3S} - \left(1+\frac{2m}{\mu_0}\right)g_{D+\frac{1}{3}F-S}\right\}\sin\theta$$

$$b_{1v} = h_F\left(1+\frac{2m}{\mu_0}\right)\left(1-\frac{t}{4m_B^2}\right)g_{D+\frac{1}{3}F-S}$$

$$d_\pm = \left(1 \pm \frac{QK}{(E_2+m_2)(E_4+m_4)}\right).$$

*Pseudoscalar exchange*

$$\phi_1 = -\mathrm{i}\tfrac{1}{2}\beta_p b_p C a_- K^2 \sin^2\theta \cos\tfrac{1}{2}\theta$$

$$\phi_2 = \mathrm{i}\beta_p b_p C a_- \frac{K}{m_3} l \sin\theta\cos\tfrac{1}{2}\theta$$

$$\phi_3 = \mathrm{i}\beta_p b_p C a_- \sqrt{\tfrac{2}{3}}\frac{1}{m_3^2}\{l^2 - \tfrac{1}{2}(m_3 K\sin\theta)^2\}\cos\tfrac{1}{2}\theta$$

$$\phi_4 = -\phi_2$$

$$\phi_5 = \phi_1$$

$$\phi_6 = \mathrm{i}\tfrac{1}{2}\beta_p b_p C a_+ K^2 \sin^2\theta \sin\tfrac{1}{2}\theta$$

$$\phi_7 = -\mathrm{i}\beta_p b_p C a_+ \frac{K}{m_3} l \sin\theta\sin\tfrac{1}{2}\theta$$

$$\phi_8 = \mathrm{i}\beta_p b_p C a_+ \sqrt{\tfrac{2}{3}}\frac{1}{m_3^2}\{l^2 - \tfrac{1}{2}(m_3 K\sin\theta)^2\}\sin\tfrac{1}{2}\theta$$

$$\phi_9 = -\phi_7$$

$$\phi_{10} = \phi_6.$$

*Vector exchange*

$$\phi_1 = \mathrm{i}\beta_v QKC\sin\theta\{-b_v KWd_-\sin\theta\cos\tfrac{1}{2}\theta + b_{1v}(-Kd_+\sin\theta\cos\tfrac{1}{2}\theta + 2a_+E_1\sin\tfrac{1}{2}\theta)\}$$

$$\phi_2 = \mathrm{i}\beta_v\frac{C}{m_3}(b_v WlQKd_-\sin\theta\cos\tfrac{1}{2}\theta + b_{1v}[lQKd_+\sin\theta\cos\tfrac{1}{2}\theta + a_+\{-2(E_1Q)^2$$
$$+E_1E_3QK(2\cos\theta - \sin^2\theta) + (E_3K)^2(\cos\theta - \cos 2\theta) - (QK\sin\theta)^2\}\sin\tfrac{1}{2}\theta])$$

$$\phi_3 = -\mathrm{i}\beta_v C\frac{2}{m_3^2}\sqrt{\tfrac{2}{3}}b_{1v}a_+K\sin\theta\sin\tfrac{1}{2}\theta(E_1E_3^2Q + \tfrac{1}{2}m_3^2E_1Q + E_3Q^2K\cos\theta$$
$$-E_3^3K\cos\theta - \tfrac{1}{2}m_3^2E_3K\cos\theta - E_1Q^3)$$

$$\phi_4 = \mathrm{i}\beta_v\frac{C}{m_3}(b_v WlQKd_-\sin\theta\cos\tfrac{1}{2}\theta + b_{1v}[lQKd_+\sin\theta\cos\tfrac{1}{2}\theta + a_+\{-E_1E_3QK$$
$$\times(2\cos\theta + \sin^2\theta) + (E_3K)^2(\cos\theta + \cos 2\theta) + (QK\sin\theta)^2\}\sin\tfrac{1}{2}\theta])$$

$$\phi_5 = -i\beta_v CK^2 \sin\theta\{-b_v WQd_- \sin\theta\cos\tfrac{1}{2}\theta + b_{1v}(-Qd_+ \sin\theta\cos\tfrac{1}{2}\theta + 2a_+E_3\sin\tfrac{1}{2}\theta)\}$$

$$\phi_6 = i\beta_v CK\sin\theta[b_v WQKd_+ \sin\theta\sin\tfrac{1}{2}\theta + b_{1v}\{QKd_- \sin\theta\sin\tfrac{1}{2}\theta + 2a_-(E_1Q - E_3K)\cos\tfrac{1}{2}\theta\}]$$

$$\phi_7 = i\beta_v\frac{C}{m_3}(-b_v WlQKd_+ \sin\theta\sin\tfrac{1}{2}\theta + b_{1v}[-lQKd_- \sin\theta\sin\tfrac{1}{2}\theta + a_+\{-2(E_1Q)^2 + E_1E_3QK(4\cos\theta + \sin^2\theta) - (E_3K)^2(\cos\theta + \cos 2\theta) - (QK\sin\theta)^2\}\cos\tfrac{1}{2}\theta])$$

$$\phi_8 = -i\beta_v C\frac{2}{m_3^2}\sqrt{\tfrac{2}{3}}b_{1v}a_-K\sin\theta\cos\tfrac{1}{2}\theta(E_1E_3Q^2 + \tfrac{1}{2}m_3^2E_1Q + E_3Q^2K\cos\theta - E_3^3K\cos\theta - \tfrac{1}{2}m_3^2E_3K\cos\theta - E_1Q^3)$$

$$\phi_9 = i\beta_v\frac{C}{m_3}(-b_v WlQKd_+ \sin\theta\sin\tfrac{1}{2}\theta + b_{1v}[-lQKd_- \sin\theta\sin\tfrac{1}{2}\theta + a_-\{E_1E_3QK\sin^2\theta - (E_3K)^2(\cos\theta - \cos 2\theta) + (QK\sin\theta)^2\}\cos\tfrac{1}{2}\theta])$$

$$\phi_{10} = -i\beta_v CQK^2\sin^2\theta\sin\tfrac{1}{2}\theta(b_v Wd_+ + b_{1v}d_-).$$

## Appendix 2

The kinematic definitions used here are the same as in appendix 1. The relations given by parity invariance are shown in table 3, and the number of independent helicity

**Table 3.** Relations between $s$ channel helicity amplitudes for $0^-\frac{1}{2}^+ \rightarrow 2^+\frac{3}{2}^+$ given by parity invariance

| $\lambda_4$ | $\lambda_3$ \ $\lambda_2\ \lambda_1$ | $\frac{1}{2}\ 0$ | $-\frac{1}{2}\ 0$ |
|---|---|---|---|
| $\frac{3}{2}$ | 2 | $\phi_1$ | $\phi_{11}$ |
| $\frac{3}{2}$ | 1 | $\phi_2$ | $\phi_{12}$ |
| $\frac{3}{2}$ | 0 | $\phi_3$ | $\phi_{13}$ |
| $\frac{3}{2}$ | $-1$ | $\phi_4$ | $\phi_{14}$ |
| $\frac{3}{2}$ | $-2$ | $\phi_5$ | $\phi_{15}$ |
| $\frac{1}{2}$ | 2 | $\phi_6$ | $\phi_{16}$ |
| $\frac{1}{2}$ | 1 | $\phi_7$ | $\phi_{17}$ |
| $\frac{1}{2}$ | 0 | $\phi_8$ | $\phi_{18}$ |
| $\frac{1}{2}$ | $-1$ | $\phi_9$ | $\phi_{19}$ |
| $\frac{1}{2}$ | $-2$ | $\phi_{10}$ | $\phi_{20}$ |
| $-\frac{1}{2}$ | 2 | $-\phi_{20}$ | $\phi_{10}$ |
| $-\frac{1}{2}$ | 1 | $\phi_{19}$ | $-\phi_9$ |
| $-\frac{1}{2}$ | 0 | $-\phi_{18}$ | $\phi_8$ |
| $-\frac{1}{2}$ | $-1$ | $\phi_{17}$ | $-\phi_7$ |
| $-\frac{1}{2}$ | $-2$ | $-\phi_{16}$ | $\phi_6$ |
| $-\frac{3}{2}$ | 2 | $\phi_{15}$ | $-\phi_5$ |
| $-\frac{3}{2}$ | 1 | $-\phi_{14}$ | $\phi_4$ |
| $-\frac{3}{2}$ | 0 | $\phi_{13}$ | $-\phi_3$ |
| $-\frac{3}{2}$ | $-1$ | $-\phi_{12}$ | $\phi_2$ |
| $-\frac{3}{2}$ | $-2$ | $\phi_{11}$ | $-\phi_1$ |

amplitudes is reduced to 20. Here, we also need the extra kinetic definitions.

$$f_p = \frac{h_{D+2S}G}{m_B}$$
$$n = E_2Q - E_4K\cos\theta$$
$$r = E_2Q + E_3\cos\theta$$
$$x = s + \tfrac{1}{2}t - \tfrac{1}{2}\sum_i m_i^2$$
$$y_1 = m_1^2 - m_3^2$$
$$y_2 = m_2^2 - m_4^2$$
$$z = \frac{Q^2 + E_3E_4}{m_4}$$
$$f_v = \frac{(1+2m/\mu_0)h_F G}{2m_B^2}$$
$$v = \frac{(2E_1+E_2)Q + E_4K\cos\theta}{m_4}.$$

*Pseudoscalar exchange*

$$\phi_1 = -\beta_p f_p \frac{Cd_-}{2\sqrt{2}}(K\sin\theta)^3\cos\tfrac{1}{2}\theta$$
$$\phi_2 = \beta_p f_p \frac{Cd_-}{\sqrt{2}m_3} l\sin^2\theta\cos\tfrac{1}{2}\theta$$
$$\phi_3 = -\beta_p f_p \frac{Cd}{\sqrt{3}m_3^2}\{l^2 - \tfrac{1}{2}(m_3K\sin\theta)^2\}\sin\theta\cos\tfrac{1}{2}\theta$$
$$\phi_4 = -\phi_2$$
$$\phi_5 = \phi_1$$
$$\phi_6 = -\beta_p f_p \frac{C}{2\sqrt{6}}(K\sin\theta)^2\left(\frac{2}{m_4}nd_-\cos\tfrac{1}{2}\theta + K\sin\theta d_+\sin\tfrac{1}{2}\theta\right)$$
$$\phi_7 = \beta_p f_p \frac{CK\sin\theta}{\sqrt{6}m_3} l\left(\frac{2}{m_4}nd_-\cos\tfrac{1}{2}\theta + K\sin\theta d_+\sin\tfrac{1}{2}\theta\right)$$
$$\phi_8 = -\beta_p f_p \frac{C}{4m_3^2}\{l^2 - \tfrac{1}{2}(m_3K\sin\theta)^2\}\left(\frac{2}{m_4}nd_-\cos\tfrac{1}{2}\theta + K\sin\theta d_+\sin\tfrac{1}{2}\theta\right)$$
$$\phi_9 = -\phi_7$$
$$\phi_{10} = \phi_6$$
$$\phi_{11} = \beta_p f_p \frac{Cd_+}{2\sqrt{2}}(K\sin\theta)^3\sin\tfrac{1}{2}\theta$$
$$\phi_{12} = -\beta_p f_p \frac{Cd_+}{\sqrt{2}m_3} l\sin^2\theta\sin\tfrac{1}{2}\theta$$

$$\phi_{13} = \beta_p f_p \frac{Cd_+}{\sqrt{3m_3^2}}\{l^2 - \tfrac{1}{2}(m_3 K \sin\theta)^2\} \sin\theta \sin\tfrac{1}{2}\theta$$

$$\phi_{14} = -\phi_{12}$$

$$\phi_{15} = \phi_{11}$$

$$\phi_{16} = \beta_p f_p \frac{C}{2\sqrt{6}}(K\sin\theta)^2\left(\frac{2}{m_4}nd_+ \sin\tfrac{1}{2}\theta - K\sin\theta d_- \cos\tfrac{1}{2}\theta\right)$$

$$\phi_{17} = -\beta_p f_p \frac{C}{\sqrt{6}m_3}K\sin\theta l_p\left(\frac{2}{m_4}nd_+ \sin\tfrac{1}{2}\theta - K\sin\theta d_- \cos\tfrac{1}{2}\theta\right)$$

$$\phi_{18} = \beta_p f_p \frac{C}{4m_3^2}\{l^2 - \tfrac{1}{2}(m_3K\sin\theta)^2\}\left(\frac{2}{m_4}nd_+ \sin\tfrac{1}{2}\theta - K\sin\theta d_- \cos\tfrac{1}{2}\theta\right)$$

$$\phi_{19} = -\phi_{17}$$

$$\phi_{20} = \phi_{16}.$$

*Vector exchange*

$$\phi_1 = -\beta_v f_v \frac{C}{\sqrt{2}}K\sin\theta\cos\tfrac{1}{2}\theta d_-[\tfrac{1}{2}(K\sin\theta)^2(-y_1+t) - x\{\tfrac{1}{2}(K\sin\theta)^2 + t\}$$
$$- y_2\{\tfrac{1}{2}(K\sin\theta)^2 + y_1\}]$$

$$\phi_2 = -\beta_v f_v \frac{C}{\sqrt{2}m_3}\cos\tfrac{1}{2}\theta d_-[(K\sin\theta)^2 r(-y_1+t) + lx\{(K\sin\theta)^2 + t\}$$
$$+ y_2\{(K\sin\theta)^2 + y_1\}]$$

$$\phi_3 = -\beta_v f_v \frac{C}{\sqrt{3m_3^2}}K\sin\theta\cos\tfrac{1}{2}\theta d_-(-\{E_1(E_1+2E_2)Q^2 - 2E_2E_3QK\cos\theta$$
$$-(E_3K\cos\theta)^2 + \tfrac{1}{2}(m_3K\sin\theta)^2\}(-y_1+t)$$
$$+x[-\{l^2 - \tfrac{1}{2}(m_3K\sin\theta)^2\} + \tfrac{1}{2}tm_3^2] + y_2[-\{l^2 - \tfrac{1}{2}(m_3K\sin\theta)^2\} + \tfrac{1}{2}m_3^2 y_1])$$

$$\phi_4 = \beta_v f_v \frac{C}{\sqrt{2}m_3}(K\sin\theta)^2\cos\tfrac{1}{2}\theta d_-\{r(-y_1+t) + l(x+y_2)\}$$

$$\phi_5 = -\beta_v f_v \frac{C}{2\sqrt{2}}(K\sin\theta)^3\cos\tfrac{1}{2}\theta d_-(-y_1+t-x-y_2)$$

$$\phi_6 = \beta_v f_v \frac{C}{\sqrt{6}}K\sin\theta\left[\tfrac{1}{2}K\sin\theta\left\{y_1\left(\frac{2n}{m_4}d_-\cos\tfrac{1}{2}\theta + K\sin\theta d_+\sin\tfrac{1}{2}\theta\right) + t(2vd_-\cos\tfrac{1}{2}\theta\right.\right.$$
$$\left. - K\sin\theta d_+\sin\tfrac{1}{2}\theta)\right\} + x\left\{\tfrac{1}{2}K\sin\theta\left(2\frac{n}{m_4}d_-\cos\tfrac{1}{2}\theta + K\sin\theta d_+\sin\tfrac{1}{2}\theta\right)\right.$$
$$\left. + td_+\sin\tfrac{1}{2}\theta\right\} + y_2\{-\tfrac{1}{2}K\sin\theta(2vd_-\cos\tfrac{1}{2}\theta - K\sin\theta d_+\sin\tfrac{1}{2}\theta)$$
$$\left. + y_1 d_+\sin\tfrac{1}{2}\theta\}\right]$$

$$\phi_7 = \beta_v f_v \frac{C}{\sqrt{6}m_3}\left[K \sin\theta r\left\{y_1\left(\frac{2n}{m_4}d_- \cos\tfrac{1}{2}\theta + K\sin\theta d_+ \sin\tfrac{1}{2}\theta\right) + t(2vd_- \cos\tfrac{1}{2}\theta\right.\right.$$

$$\left. - K\sin\theta d_+ \sin\tfrac{1}{2}\theta)\right\} + x\left\{-K\sin\theta l\left(\frac{2n}{m_4}d_- \cos\tfrac{1}{2}\theta + K\sin\theta d_+ \sin\tfrac{1}{2}\theta\right)\right.$$

$$\left. - t(zK\sin\theta d_- \cos\tfrac{1}{2}\theta + ld_+ \sin\tfrac{1}{2}\theta)\right\} + y_2\left\{K\sin\theta l\left(\frac{2n}{m_4}d_- \cos\tfrac{1}{2}\theta\right.\right.$$

$$\left.\left. - K\sin\theta d_+ \sin\tfrac{1}{2}\theta) - y_1(zK\sin\theta d_- \cos\tfrac{1}{2}\theta + ld_+ \sin\tfrac{1}{2}\theta)\right\}\right]$$

$$\phi_8 = -\beta_v f_v \frac{C}{3m_3^2}\left[\{E_1(E_1+2E_2)Q^2 - 2E_2E_3QK\cos\theta - (E_3K\cos\theta)^2 + \tfrac{1}{2}(m_3K\sin\theta)^2\}\right.$$

$$\times\left\{y_1\left(2\frac{n}{m_4}d_- \cos\tfrac{1}{2}\theta + K\sin\theta d_+ \sin\tfrac{1}{2}\theta\right) + t(2vd_- \cos\tfrac{1}{2}\theta - K\sin\theta d_+\right.$$

$$\left.\times \sin\tfrac{1}{2}\theta)\right\} + x\left\{-\{l^2 - \tfrac{1}{2}(m_3K\sin\theta)^2\}\left(\frac{2n}{m_4}d_- \cos\tfrac{1}{2}\theta + K\sin\theta d_+ \sin\tfrac{1}{2}\theta\right)\right.$$

$$\left. + t\left(-2\frac{2zl}{m_3^2}d_- \cos\tfrac{1}{2}\theta + \tfrac{1}{2}K\sin\theta d_+ \sin\tfrac{1}{2}\theta\right)\right\} + y_2\left\{\{l^2 - \tfrac{1}{2}(m_3K\sin\theta)^2\}\right.$$

$$\times(2vd_- \cos\tfrac{1}{2}\theta - K\sin\theta d_+ \sin\tfrac{1}{2}\theta) + y_1\left(-2\frac{zl}{m_3^2}d_- \cos\tfrac{1}{2}\theta + \tfrac{1}{2}K\sin\theta\right.$$

$$\left.\left.\left.\times d_+ \sin\tfrac{1}{2}\theta\right)\right\}\right]$$

$$\phi_9 = -\beta_v f_v \frac{CK\sin\theta}{\sqrt{6}m_3}\left[r\left\{y_1\left(\frac{2n}{m_4}d_- \cos\tfrac{1}{2}\theta + K\sin\theta d_+ \sin\tfrac{1}{2}\theta\right) + t(2vd_- \cos\tfrac{1}{2}\theta\right.\right.$$

$$\left. - K\sin\theta d_+ \sin\tfrac{1}{2}\theta)\right\} - x\left\{l\left(\frac{2n}{m_4}d_- \cos\tfrac{1}{2}\theta + K\sin\theta d_+ \sin\tfrac{1}{2}\theta\right)\right.$$

$$\left.\left. + tzd_- \cos\tfrac{1}{2}\theta\right\} - y_2\{-l(2vd_- \cos\tfrac{1}{2}\theta - K\sin\theta d_+ \sin\tfrac{1}{2}\theta) + y_1zd_- \cos\tfrac{1}{2}\theta\}\right]$$

$$\phi_{10} = \beta_v f_v \frac{C(K\sin\theta)^2}{2\sqrt{6}}\left\{y_1\left(\frac{2n}{m_4}d_- \cos\tfrac{1}{2}\theta + K\sin\theta d_+ \sin\tfrac{1}{2}\theta\right) + t(2vd_- \cos\tfrac{1}{2}\theta\right.$$

$$- K\sin\theta d_+ \sin\tfrac{1}{2}\theta) + x\left(\frac{2n}{m_4}d_- \cos\tfrac{1}{2}\theta + K\sin\theta d_+ \sin\tfrac{1}{2}\theta\right) - y_2(2vd_- \cos\tfrac{1}{2}\theta$$

$$\left. - K\sin\theta d_+ \sin\tfrac{1}{2}\theta)\right\}$$

$$\phi_{11} = \beta_v f_v \frac{C}{\sqrt{2}}K\sin\tfrac{1}{2}\theta d_+[\tfrac{1}{2}(K\sin\theta)^2(-y_1+t) - x\{\tfrac{1}{2}(K\sin\theta)^2 + t\}$$

$$- y_2\{\tfrac{1}{2}(K\sin\theta)^2 + y_1\}]$$

$$\phi_{12} = \beta_v f_v \frac{C}{\sqrt{2}m_3}\sin\tfrac{1}{2}\theta d_+((K\sin\theta)^2 r(-y_1+t) + l[x\{(K\sin\theta)^2 + t\}$$

$$+ y_2\{(K\sin\theta)^2 + y_1\}])$$

$$\phi_{13} = \beta_v f_v \frac{C}{\sqrt{3m_3^2}} K \sin\theta \sin\tfrac{1}{2}\theta d_+ (-\{E_1(E_1+2E_2)Q^2 - 2E_2E_3QK\cos\theta - (E_3K\cos\theta)^2$$
$$+\tfrac{1}{2}(m_3K\sin\theta)^2\}(-y_1+t) + x[-\{l^2-\tfrac{1}{2}(m_3K\sin\theta)^2\}+\tfrac{1}{2}tm_3^2]$$
$$+y_2[-\{l^2-\tfrac{1}{2}(m_3K\sin\theta)^2\}+\tfrac{1}{2}m_3^2y_1])$$

$$\phi_{14} = -\beta_v f_v \frac{C}{\sqrt{2m_3}}(K\sin\theta)^2 \sin\tfrac{1}{2}\theta d_+\{r(-y_1+t)+l(x+y_2)\}$$

$$\phi_{15} = \beta_v f_v \frac{C}{2\sqrt{2}}(K\sin\theta)^3 \sin\tfrac{1}{2}\theta d_+(-y_1+t-x-y_2)$$

$$\phi_{16} = -\beta_v f_v \frac{C}{\sqrt{6}} K\sin\theta\left[\tfrac{1}{2}K\sin\theta\left\{y_1\left(\frac{2n}{m_4}d_+\sin\tfrac{1}{2}\theta - K\sin\theta d_-\cos\tfrac{1}{2}\theta\right)+t(2vd_+\sin\tfrac{1}{2}\theta\right.\right.$$
$$\left.+K\sin\theta d_-\cos\tfrac{1}{2}\theta)\right\} + x\left\{\tfrac{1}{2}K\sin\theta\left(2\frac{n}{m_4}d_+\sin\tfrac{1}{2}\theta - K\sin\theta d_-\cos\tfrac{1}{2}\theta\right)\right.$$
$$\left.-td_-\cos\tfrac{1}{2}\theta\right\} + y_2\{-\tfrac{1}{2}K\sin\theta(2vd_+\sin\tfrac{1}{2}\theta + K\sin\theta d_-\cos\tfrac{1}{2}\theta)$$
$$\left.-y_1d_-\cos\tfrac{1}{2}\theta\}\right]$$

$$\phi_{17} = -\beta_v f_v \frac{C}{\sqrt{6m_3}}\left[K\sin\theta\left\{y_1\left(\frac{2n}{m_4}d_+\sin\tfrac{1}{2}\theta - K\sin\theta d_-\cos\tfrac{1}{2}\theta\right)+t(2vd_+\sin\tfrac{1}{2}\theta\right.\right.$$
$$\left.+K\sin\theta d_-\cos\tfrac{1}{2}\theta)\right\} - x\left\{K\sin\theta l\left(\frac{2n}{m_4}d_+\sin\tfrac{1}{2}\theta - K\sin\theta d_-\cos\tfrac{1}{2}\theta\right)\right.$$
$$\left.+t(zK\sin\theta d_+\cos\tfrac{1}{2}\theta - ld_-\sin\tfrac{1}{2}\theta)\right\} + y_2\left\{K\sin\theta l\left(\frac{2n}{m_4}d_+\sin\tfrac{1}{2}\theta\right.\right.$$
$$\left.\left.\left.+K\sin\theta d_-\cos\tfrac{1}{2}\theta\right) - y_1(zK\sin\theta d_+\sin\tfrac{1}{2}\theta - ld_-\cos\tfrac{1}{2}\theta)\right\}\right]$$

$$\phi_{18} = \beta_v f_v \frac{C}{3m_3^2}\left[\{E_1(E_1+2E_2)Q^2 - 2E_2E_3QK\cos\theta - (E_3K\cos\theta)^2 + \tfrac{1}{2}(m_3K\sin\theta)^2\}\right.$$
$$\times\left\{y_1\left(\frac{2n}{m_4}d_+\sin\tfrac{1}{2}\theta - K\sin\theta d_-\cos\tfrac{1}{2}\theta\right)+t(2vd_+\sin\tfrac{1}{2}\theta + K\sin\theta d_-\right.$$
$$\left.\times\cos\tfrac{1}{2}\theta)\right\} - x\left\{\{l^2-\tfrac{1}{2}(m_3K\sin\theta)^2\}\left(\frac{2n}{m_4}d_+\sin\tfrac{1}{2}\theta - K\sin\theta d_-\cos\tfrac{1}{2}\theta\right)\right.$$
$$\left.\left.-t\left(\frac{2zl}{m_3^2}d_+\sin\tfrac{1}{2}\theta + K\sin\theta d_-\cos\tfrac{1}{2}\theta\right)\right\}\right]$$

$$\phi_{19} = \beta_v f_v \frac{C}{\sqrt{6m_3}} K\sin\theta\left[r\left\{y_1\left(\frac{2n}{m_4}d_+\sin\tfrac{1}{2}\theta - K\sin\theta d_-\cos\tfrac{1}{2}\theta\right)+t(2vd_+\sin\tfrac{1}{2}\theta\right.\right.$$
$$\left.+K\sin\theta d_-\cos\tfrac{1}{2}\theta)\right\} - x\left\{l\left(\frac{2n}{m_4}d_+\sin\tfrac{1}{2}\theta - K\sin\theta d_-\cos\tfrac{1}{2}\theta\right)\right.$$
$$\left.\left.+tzd_+\sin\tfrac{1}{2}\theta\right\} - y_2\{-l(2vd_+\sin\tfrac{1}{2}\theta + K\sin\theta d_-\cos\tfrac{1}{2}\theta) + y_1zd_+\sin\tfrac{1}{2}\theta\}\right]$$

$$\phi_{20} = -\beta_v f_v \frac{C}{2\sqrt{6}}(K\sin\theta)^2 \left[\left\{y_1\left(\frac{2n}{m_4}d_+ \sin\tfrac{1}{2}\theta - K\sin\theta d_- \cos\tfrac{1}{2}\theta\right) + t(2vd_+ \sin\tfrac{1}{2}\theta + K\sin\theta d_- \cos\tfrac{1}{2}\theta)\right\} + x\left(\frac{2n}{m_4}d_+ \sin\tfrac{1}{2}\theta - K\sin\theta d_- \cos\tfrac{1}{2}\theta\right) - y_2(2vd_+ \sin\tfrac{1}{2}\theta + K\sin\theta d_- \cos\tfrac{1}{2}\theta)\right].$$

**Table 4.** Clebsch–Gordan coefficients for $0^-\frac{1}{2}^+ \to 2^+\frac{1}{2}^+$

| | | Baryon | Vertex | Meson | Vertex |
|---|---|---|---|---|---|
| Reaction | Exchange | $F+3S$ | $D+\frac{2}{3}F-S$ | $D+2S$ | $F$ |
| $\pi^-p \to f^0n$ | $\pi$ | $\sqrt{2}$ | $5\sqrt{2}/3$ | 2 | |
| $K^-p \to K^{**-}p$ | $\pi$ | $+1$ | $5/3$ | $+1$ | |
| | $\rho$ | $+1$ | $5/3$ | | $-1$ |
| | $\omega$ | 3 | $-1/3$ | | $-1$ |
| | $f^0$ | 3 | $-1/3$ | $+1$ | |
| $K^-p \to \bar{K}^{**0}n$ | $\pi$ | $\sqrt{2}$ | $5\sqrt{2}/3$ | $\sqrt{2}$ | |
| | $\rho$ | $\sqrt{2}$ | $5\sqrt{2}/3$ | | $-\sqrt{2}$ |
| $\pi^+p \to A_2^+p$ | $\rho$ | 1 | $5/3$ | | 2 |
| | $f^0$ | 3 | $-1/3$ | 2 | |
| $\pi^-p \to A_2^-p$ | $\rho$ | 1 | $5/3$ | | $-2$ |
| | $f^0$ | 3 | $-1/3$ | 2 | |

**Table 5.** Clebsch–Gordan coefficients for $0^-\frac{1}{2}^+ \to 2^+\frac{3}{2}^+$

| | | Baryon vertex | Meson | Vertex |
|---|---|---|---|---|
| Reaction | Exchange | $G$ | $D+2S$ | $F$ |
| $\pi^+p \to f^0\Delta^{++}$ | $\pi$ | $-\sqrt{2}$ | 2 | |
| $\pi^+p \to A_2^0\Delta^{++}$ | $\rho$, B | $-\sqrt{2}$ | | 2 |

## References


Aachen, Berlin, Birmingham, Bonn, Hamburg, London (IC) and München Collaboration 1965 *Phys. Rev.* **138** B897

Aachen, Birmingham, Bonn, Hamburg, London (IC) and München Collaboration 1964 *Nuovo Cim.* **31** 729

Aachen, Berlin and CERN Collaboration 1966 *Phys. Lett.* **22** 533

—— 1968 *Nucl. Phys.* B **8** 45

—— 1970 *Nucl. Phys.* B **24** 509

Aachen, Berlin, CERN, London (IC) and Vienna Collaboration *Nucl. Phys.* B **7** 111

—— 1971 *Ann. Phys.* to be published

—— 1972 *Nucl. Phys.* B **39** 201

Adjei S A *et al* 1970 *Computational Physics: Inst. Phys. Digest No* 2 p 57

Birmingham, Glasgow, London (IC), München, Oxford and Rutherford Laboratory Collaboration 1968 *Nuovo Cim.* A **53** 522

Biswas N N *et al* 1970 *Phys. Rev.* D **2** 2529

Caso C *et al* 1969 *Nuovo Cim.* A **62** 755

Delbourgo R, Rashid M A, Salam A and Strathdee J 1965 *Seminar on High-Energy Physics and Elementary Particles, Trieste* (Vienna: International Atomic Energy Agency)
Ebel G, Pulkuhn H and Steiner F 1969 *Proc. Int. Conf. on Elementary Particles, Israel*
Flaminio B, Hansen J, Morrison D R O and Tovey N 1970 *CERN-HERA Report No* 70–6, 70–7
Freund P G O, Jones H F and Rivers R J 1971 *Phys. Lett.* **36B** 89
Gaidos J A, Ezell C R, Lamsa J W and Willmann R B 1971 *Nucl. Phys.* B **26** 225
Grayer G *et al* 1971 *Phys. Lett.* **34B** 333
Jackson J D *et al* 1965 *Phys. Rev.* **139** B428
Johnson T F *et al* 1970 *Nucl. Phys.* B **24** 253
Lovelace C 1971 *Proc. Cal. Tech. Conf.*, March 1971
Michael C and Runskanen P V 1971 *CERN Report No* TH1308-CERN
Particle Data Group 1970 *Rev. mod. Phys.* **42** 87
Phillips R J N 1970 *Proc. 9th Int. Universitätswochen für Kernphysik der Universität Schladming* (Vienna: Springer-Verlag)
Pilkuhn H and Svensson B E Y 1965 *Nuovo Cim.* **38** 518
Poirier J A *et al* 1967 *Phys. Rev.* **163** 1462
Schweingruber *et al* 1968 *Phys. Rev.* **166** 1317